

Nanoparticle-based Endodontic Antimicrobial Photodynamic Therapy

Tom C. Pagonis, DDS, MS,* Judy Chen, DDS,* Carla Raquel Fontana, DDS, PhD,[†] Harikrishna Devalapally, PhD,[‡] Karriann Ruggiero, BS,[†] Xiaoqing Song, MD, MS,[†] Federico Foschi, DDS, PhD,[†] Joshua Dunham, BS,[†] Ziedonis Skobe, PhD,[‡] Hajime Yamazaki, MS,[‡] Ralph Kent, ScD,^{||} Anne C.R. Tanner, BDS, PhD,[§] Mansoor M. Amiji, PhD,[¶] and Nikolaos S. Soukos, DDS, PhD[#]

Abstract

Objective: To study the *in vitro* effects of poly(lactico-glycolic acid) (PLGA) nanoparticles loaded with the photosensitizer methylene blue (MB) and light against *Enterococcus faecalis* (ATCC 29212). **Materials and Methods:** The uptake and distribution of nanoparticles in *E. faecalis* in suspension was investigated by transmission electron microscopy (TEM) after incubation with PLGA complexed with colloidal gold particles for 2.5, 5, and 10 minutes. *E. faecalis* species were sensitized in planktonic phase and in experimentally infected root canals of human extracted teeth with MB-loaded nanoparticles for 10 minutes followed by exposure to red light at 665 nm. **Results:** The nanoparticles were found to be concentrated mainly on the cell walls of microorganisms at all three time points. The synergism of light and MB-loaded nanoparticles led to approximately 2 and 1 log₁₀ reduction of colony-forming units (CFUs) in planktonic phase and root canals, respectively. In both cases, mean log₁₀ CFU levels were significantly lower than controls and MB-loaded nanoparticles without light. **Conclusion:** The utilization of PLGA nanoparticles encapsulated with photoactive drugs may be a promising adjunct in antimicrobial endodontic treatment. (*J Endod* 2010;36:322–328)

Key Words

Endodontic disinfection, *Enterococcus faecalis*, methylene blue, photodynamic therapy, polymeric nanoparticles

The goal of endodontic treatment is to prevent and, when required, to eliminate endodontic infection and allow healing of apical periodontitis (1). Although the bulk of the infecting microorganisms are removed during chemomechanical debridement, residual bacteria are readily detectable in approximately one half of teeth at the time of obturation (2). The complexity of the root canal system with its isthmuses, ramifications, and dentinal tubules make complete debridement of bacteria almost impossible, even when conventional methods of endodontic instrumentation and irrigation are performed to the highest technical standards (3). Furthermore, scanning electron microscopic investigations have shown bacterial penetration up to 1,000 μm into dentinal tubules (4). The presence of a “smear layer” during and after instrumentation reduces the effectiveness of irrigants and intracanal medicaments in disinfecting dentinal tubules (5). Nonsurgical endodontic treatment failures are associated with high proportions of gram-positive aerobic and facultative organisms versus the predominance of strict anaerobes in primary endodontic infections (6, 7). *Enterococcus faecalis* microorganisms, which are rarely found in large proportions in primary endodontic infections, are highly associated with endodontic failures (8, 9) and show resistance to common intracanal medications (10). Disinfection of the root canal system is critical to success, and the need for better root canal disinfection is clear and compelling.

The use of photodynamic therapy (PDT) for the inactivation of microorganisms was first shown more than 100 years ago when Oscar Raab reported the lethal effect of acridine hydrochloride on *Paramecia caudatum* (11). PDT is based on the concept that nontoxic photosensitizers can be preferentially localized in certain tissues and subsequently activated by light of the appropriate wavelength to generate singlet oxygen and free radicals that are cytotoxic to cells of the target tissue (12). Methylene blue (MB) is a well-established photosensitizer that has been used in PDT for targeting various gram-positive and gram-negative oral bacteria (13) and was previously used to study the effect of PDT on endodontic disinfection (14–20). Several studies have shown incomplete destruction of oral biofilms using MB-mediated PDT (21–24). The reduced susceptibility of biofilms to PDT was attributed to reduced penetration of the photosensitizer (21, 22). In addition, it has been shown that phenothiazinium-based photosensitizers, including MB and toluidine blue O, are substrates of

From *Advanced Graduate Endodontics, Division of Endodontics, Harvard School of Dental Medicine, Boston, Massachusetts; [†]Applied Molecular Photomedicine Laboratory, The Forsyth Institute, Boston, Massachusetts; [‡]Department of Biomineralization, The Forsyth Institute, Boston, Massachusetts; [§]Department of Molecular Genetics, The Forsyth Institute, Boston, Massachusetts; ^{||}Department of Biostatistics, The Forsyth Institute, Boston, Massachusetts; [¶]Department of Pharmaceutical Sciences, School of Pharmacy, Bouvé College of Health Sciences, Northeastern University, Boston, Massachusetts; [#]Applied Molecular Photomedicine Laboratory, The Forsyth Institute, Boston, Massachusetts.

Supported by NIDCR grant R01-DE-16922.

Address requests for reprints to Dr Nikolaos Soukos, Applied Molecular Photomedicine Laboratory, The Forsyth Institute, 140 The Fenway, Boston, MA 02115-3799.

E-mail address: nsoukos@forsyth.org.

0099-2399/\$0 - see front matter

Copyright © 2010 American Association of Endodontists.

doi:10.1016/j.joen.2009.10.011

multidrug resistance pumps in bacteria, thus decreasing the effectiveness of the photosensitizer (25). Therefore, one of the ways to overcome these deficiencies is to develop drug delivery systems that significantly improve the pharmacological characteristics of MB.

Recently, studies in PDT have focused on the use of polymer-based nanoparticles for photosensitizer delivery and release systems. Nanoparticles containing photosensitizers have several advantages over photosensitizing molecules not encapsulated in nanoparticles. These advantages include (26) (1) a larger critical mass (concentrated package of photosensitizer) for the production of reactive oxygen species that destroy cells; (2) limiting the target cell's ability to pump the drug molecule back out, thus reducing the possibility of multiple-drug resistance; (3) selectivity of treatment by localized delivery agents, which can be achieved by either passive targeting or by active targeting via the charged surface of the nanoparticle, and (4) the nanoparticle matrix is nonimmunogenic. Engineered biodegradable polymeric nanoparticles, made of Food and Drug Administration–approved poly(lactic-co-glycolic acid) (PLGA) (27), were used as a drug delivery system for photosensitizers (28–30). Once encapsulated within PLGA, the excited state of the photosensitizer is quenched, which results in a loss of phototoxicity (29). When the nanoparticles were incubated with the targeted cells, they showed a time-dependent release of the photosensitizer, which then regained its phototoxicity and resulted in an activatable PDT nanoagent (29). Although PLGA nanoparticles loaded with various compounds (eg, antibiotics) have been used for bacterial targeting (31, 32), the use of PLGA nanoparticles as carriers of photosensitizers has not been previously explored in antimicrobial PDT.

The objective of the present study was to use MB-loaded PLGA nanoparticles for *in vitro* evaluations against *E. faecalis*. We also explored the photodynamic effects of these nanoparticles in targeting *E. faecalis* biofilms in experimentally infected root canals of extracted teeth. Our hypothesis was that the encapsulation of MB within PLGA nanoparticles (~150–200 nm in diameter) may offer a novel design of a nanopatform for enhanced drug delivery in the root canal system and photodestruction of root canal biofilms.

Materials and Methods

Preparation of PLGA Nanocarriers

Medical grade PLGA (molecular weight of 12 Kd, 50:50 lactide-glycolide molar ratio) was obtained from Birmingham Polymers (Pelham, AL). Pluronic F-108, an ABA triblock copolymer of poly(ethylene oxide) (PEO) and poly(propylene oxide), was kindly supplied by the Performance Chemicals Division of BASF Corporation (Parsippany, NJ). Both blank and MB-loaded (10% w/w) PLGA nanoparticles were prepared by blending the polyester with Pluronic F-108 triblock copolymer and fabricating the nanoparticles by a solvent displacement procedure as previously reported (33). Briefly, a solution of PLGA (76 mg) and Pluronic F-108 (14 mg) was prepared in acetone (5 mL) and heated with stirring until it became clear. This was introduced into an aqueous (50 mL) solution under vigorous magnetic stirring. The rate of addition of organic phase (1 mL/min) to aqueous phase, volume ratios, and the stirring speed was optimized to ensure batch-to-batch reproducibility. After overnight stirring, the nanoparticle was centrifuged at 10,000 rpm for 20 minutes and then washed twice with water and freeze dried. For the preparation of the nanocarrier formulations, MB and sodium oleate were purchased from Sigma Chemicals (St Louis, MO). The oleate salt of MB was dissolved at 10% (w/w) concentration in the acetone solution of PLGA. Pluronic triblock copolymers were added to the polymer solution in acetone at 20% (w/w). The concentration and type of Pluronic triblock copolymer was optimized to ensure that

the formed nanocarriers have a stable hydrophilic surface, which resists aggregation.

Characterization of PLGA Nanocarriers

The mean size of PLGA nanoparticles, with and without the encapsulated payloads, was determined via laser light scattering using a Zeta-PALS system (Brookhaven Instruments, Holtsville, NY). After freeze-drying, the surface morphology of the nanocarriers was visualized using field emission scanning electron microscopy (Shimadzu, Japan). The surface charge on the nanocarriers, in the absence and presence of encapsulated payload, was determined by zeta potential measurements. Zeta potential measurements of the nanocarrier suspensions in phosphate-buffered saline (PBS, pH = 7.4) were performed with Brookhaven Instruments and ZetaPALS (Phase Analysis Light Scattering) ultra-sensitive zeta potential analyzer. To determine the amount of drug loaded into the nanocarriers (capacity) as well as the percentage of added drug (efficiency), a known amount (~10 mg) of the control and PEO-modified nanocarriers was dissolved in acetone. The amount of encapsulated drug in the nanocarriers was determined by using the ultraviolet-visible spectroscopy (UV-VIS) absorbance of MB. The release kinetics of MB-oleate from the nanoparticles was determined in PBS (pH = 7.4). Tween-80, a nonionic surfactant at 1.0% (w/v) concentration, was added to the release medium to enhance the solubility of MB-oleate complex and to prevent the drugs from binding to the container surface. One hundred milligrams of the drug-containing nanocarriers was incubated with 10 mL of the release medium in a shaking water bath (50 rpm). Periodically, 5 mL of the release medium was removed and replaced with 5 mL of fresh buffer to maintain sink conditions. MB in the release medium was assayed by a Shimadzu UV-VIS spectrophotometer (Columbia, MD). Cumulative amount and percent drug released was determined from appropriate calibration curves of the respective agents.

Bacterial Culture

Enterococcus faecalis (ATCC 29212) was used in this study. Cultures were maintained by weekly subculture in plates comprised of trypticase soy agar (Becton, Dickinson, and Co, Sparks, MD) with 5% sheep blood (Northeast Laboratories, Waterville, ME). For experimental purposes, the microorganism was grown in the presence of 80% N₂, 10% H₂, 10% CO₂ at 35°C in an anaerobic chamber for 72 hours; harvested from plates; and resuspended in brain heart infusion (BHI) broth. Cells were dispersed by vortexing and repeated passage through Pasteur pipettes. Cell numbers were measured in a spectrophotometer (wavelength, 600 nm; 0.1 optical density unit equals approximately 10⁸ cells/mL) in 1-mL cuvettes.

Bacterial Uptake of Nanoparticles

The uptake and distribution in *E. faecalis* was investigated by transmission electron microscopy (TEM) using PLGA complexed with colloidal gold particles. Colloidal gold nanoparticles (10–15 nm) were prepared by a reduction of chloroauric acid with sodium citrate. To a flask containing 85 mL of boiling high-performance liquid chromatography (HPLC) water, chloroauric acid (HAuCl₄) solution (10 mL, 5 mmol/L) was added, and the solution was allowed to return to a boil. A freshly prepared solution of sodium citrate (5 mL, 0.03 mol/L) was then added to the flask. After a few minutes, the solution turned from colorless to a deep wine-red color. Heating was stopped at this point, and the resulting sol was left to cool overnight. The nanoparticles were centrifuged at 30,000 rpm for 10 minutes, and the supernatant was discarded. The remaining pellet was redispersed in deionized distilled water for further use. The physical properties of the

nanoparticles, such as size and zeta potential, were compared with those of unloaded nanoparticles and were not found to be significantly different. Bacteria (10^8 /mL) were incubated with PLGA-Au-Pluronic nanoparticle suspension (100 μ g/mL) for 2.5, 5, and 10 minutes, centrifuged, and washed twice with PBS. Then, microorganisms were fixed in 2.5% glutaraldehyde solution at room temperature for 1 hour, washed with distilled water, and postfixed in 1% osmium tetroxide and uranyl acetate. The cells were dehydrated with ethanol and embedded in Embed® 812 (Electron Microscopy Sciences, Hatfield, PA). Thin-sectioned samples were prepared and examined using a transmission electron microscope (JEOL JEM-1200 EX, Peabody, MA).

Photodynamic Treatment of Bacterial Suspensions

For the photodynamic treatment of microorganisms, aliquots of bacterial suspensions (10^8 /mL) were placed in sterile microcentrifuge tubes and were centrifuged (7,000 rpm for 4 minutes). The supernatants were aspirated and 1 mL of BHI with MB-loaded PLGA nanoparticles (final concentration: 6.25 μ g/mL equivalent to MB) was then added. Cultures were resuspended with the nanoparticles and placed in the wells of 24-well plates for 10 minutes before they were exposed to light. All wells were irradiated with red light from a diode laser (BWTEK Inc, Newark, DE) with an output power of 1 W and a central wavelength of 665 nm for 10 minutes in the dark at room temperature. The system was coupled to an optical fiber 1 mm in diameter that delivered light into a lens. This formed a uniform circular spot on the base of the 24-well plate, 2 cm in diameter. The laser possessed a spectral stability of ± 2 nm with an output power stability of 10 mW. Power measurements were quantified with a power meter (Ophir Optonics LTD, Danvers, MA). Distance adjustments between the lens and the illuminated plates created fields of irradiation with appropriate dimensions and power densities. The light exposure was from above with an irradiance of 100 mW/cm² and an energy fluence of 60 J/cm². All plates were kept covered during the illumination in order to maintain the purity of the culture. After illumination of the appropriate wells, bacterial suspensions underwent serial dilutions in BHI broth, and 100- μ L aliquots were plated on blood agar plates for anaerobic incubation for 7 days. The following experimental groups were used: (1) no light/no MB nanoparticles (control), (2) treated only with MB-loaded nanoparticles, and (3) treated with MB-loaded nanoparticles and light. Three separate experiments were performed with four bacterial cultures per group in each experiment. The primary endpoint for evaluation was the mean number of colony-forming units (CFUs) per group.

Preparation of Tooth Specimens

Thirty-two freshly extracted single-rooted human teeth were stored in 0.5% sodium hypochlorite (NaOCl) for 2 weeks. Specimens were decoronated to a standard 12-mm root segment length with a rotating diamond saw (#911H; Brasseler USA, Savannah, GA) set at 20,000 rpm under water coolant. Patency of apical foramina was established by inserting a size 15 K-file (Dentsply Maillefer, Tulsa, OK). A file measurement was taken at the point in which the size 15 K-file became visible at the apical foramen and 0.5 mm was subtracted to set the working length. The instrumentation sequence consisted of Gates Glidden Burs (Dentsply Maillefer, Tulsa, OK) sizes 4 and 2 for the coronal 4 mm and ProTaper S1 (Dentsply Tulsa Dental, Tulsa, OK) followed by .06 taper Profile series 29 (Dentsply Tulsa Dental, Tulsa, OK) files sizes 4 (0.216 International Organization for Standardization [ISO] equivalent) to 7 (0.465 ISO equivalent) in a crown-down manner to achieve a master apical file size of 0.465 (ISO equivalent). An Aseptico Endo ITR (Dentsply Tulsa Dental, Tulsa, OK) electric motor was used with an 8:1 gear reduction minihead contra-angle. Final apical patency was estab-

lished with a size 25 K-file (Dentsply Maillefer) in order to allow for an adequate apical aperture for flushing of microbial aggregates. RC Prep (Premium Products, Plymouth Meeting, PA) was used as a lubricant, and canals were irrigated with 6% sodium hypochlorite (NaOCl) throughout the instrumentation sequence. The final canal irrigation consisted of 1 mL of 17% EDTA solution for 3 minutes for smear layer removal that was deactivated with 1 mL of 6% NaOCl for 3 minutes. Each tooth specimen was then placed in a microcentrifuge tube containing 500 μ L of PBS. Teeth were subsequently autoclaved at 121°C for 20 minutes. After autoclave sterilization, PBS was aspirated from the microcentrifuge tubes under sterile conditions. The root surface was coated with Performix (Plasti Dip, Blaine, MN) to avoid external microbial contamination.

Infection of Root Canals

Twenty-six root specimens were transferred into sterile microcentrifuge tubes under sterile conditions. One milliliter of BHI broth containing 10^9 microorganisms of *E. faecalis* was injected into the prepared root canal system using a ProRinse 30-G irrigation needle (Dentsply Tulsa Dental). After injection, each specimen was entirely submerged in BHI broth, and the tubes were incubated anaerobically for 3 days. After incubation, the medium was aseptically aspirated from the tubes. Three specimens were processed for scanning electron microscopy (SEM) studies, and 23 specimens were used for PDT studies.

SEM

A total of nine human extracted teeth with a single canal were randomly selected for SEM. Three specimens were used for demonstration of the smear layer removal and the patency of dentinal tubules and three specimens for the demonstration of *E. faecalis* infection. The root canals of three uninfected specimens were incubated with 1 mL of PBS containing MB-loaded nanoparticles (final concentration: 50 μ g/mL equivalent to MB) for 15 minutes to show the delivery of nanoparticles in the root canal system. Longitudinal grooves were cut with a diamond bur both on palatal/lingual and buccal surfaces of each root to facilitate vertical splitting with a chisel. Each sample was split into two halves with a stainless steel chisel. The sample half with the most visible part of the apex was fixed in 3.7% glutaraldehyde in 0.2 mol/L of sodium cacodylate-buffered solution at 4°C for 24 hours. After dehydration in a graded ethanol concentration series, samples were air dried and mounted on SEM stubs for gold sputtering and observation with a JEOL JSM 6400 scanning electron microscope (JEOL Corporation, Tokyo, Japan). SEM microphotographs were obtained at a standard magnification of 1,500 \times at each third (coronal, middle, and apical) and on the fracture surface.

Photodynamic Treatment of Root Canal Biofilms

Twenty-three root specimens were prepared and infected as described previously and were subjected to PDT using MB-loaded nanoparticles in BHI broth. The specimens were randomly assigned to the following three groups: (1) no light/no MB nanoparticles, (2) treated only with MB-loaded nanoparticles, and (3) treated with MB-loaded nanoparticles and light. Two separate experiments were performed with four specimens per group in each experiment with the exception of the group treated only with MB-loaded nanoparticles, in which 4 and 3 specimens were used, respectively. All individual specimens were placed in 1.5-mL microcentrifuge tubes under sterile conditions, and then the canals of the MB-loaded nanoparticles only and PDT groups were filled to the level of the access cavity with nanoparticle solution (final concentration: 50 μ g/mL equivalent to MB) using a Pro Rinse

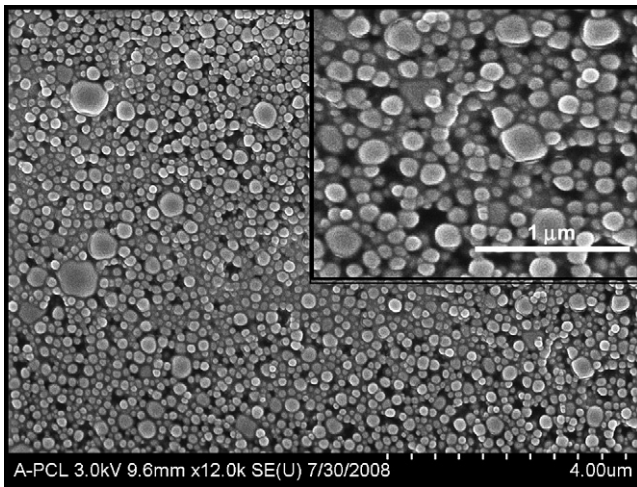


Figure 1. SEM of blank PLGA nanoparticles. The inset shows an SEM image of higher magnification with spherical nanoparticles of 150 to 250 nm in diameter.

30-G irrigation needle (Dentsply Tulsa Dental). After injection, the entire specimen was fully immersed in the solution for 15 minutes so that the root canal system will be continuously exposed to the drug. In a clinical setting, the drug will be applied in the root canal and taken up by

residual bacteria in the main root canal, isthmuses, lateral canals, and dentinal tubules. To minimize the *in vitro* impact of the drug escaping from the apex, we attempted to mimic the continuous *in vivo* clinical presence of the drug during nonsurgical endodontic treatment by fully immersing the root specimen in the drug solution in order to provide the continuous intracanal presence of MB. In addition, the Performix coating eliminated any possible seepage of MB from the root surface. Specimens in the control groups were injected and fully immersed in sterile BHI broth. After incubation, excess drug solution was aspirated, and the root specimens were removed from the tubes. Light was then applied in the root canal system of the specimens for 5 minutes. The irradiation source was a diode laser (BWTEK Inc, Newark, DE) with an output power of 1 W and a central wavelength of 665 nm. The system was coupled to a 250- μ m diameter poly(methylmethacrylate) optical fiber that was mechanically notched over a 1-cm length at approximately 1-mm intervals (Schoelly Imaging Inc, Worcester, MA). The fiber was able to uniformly distribute light at 360° (18). The power density was 100 mW/cm², and the total energy fluence dose was 30 J/cm². After all treatments, each specimen was aseptically mounted on a rubber dam by utilizing a plastic u-shaped rubber dam frame (Hygienic Brand; Coltene/Whaledent, Cuyahoga Falls, OH) attached to a rack and oriented parallel to the lab bench top. The coronal 4 mm of each specimen was above the surface of the dam. The contents of root canals were sampled by flushing the root canals with a coronal application of 1 mL of BHI broth with a Pro Rinse 30-G irrigation needle (Dentsply Tulsa Dental).

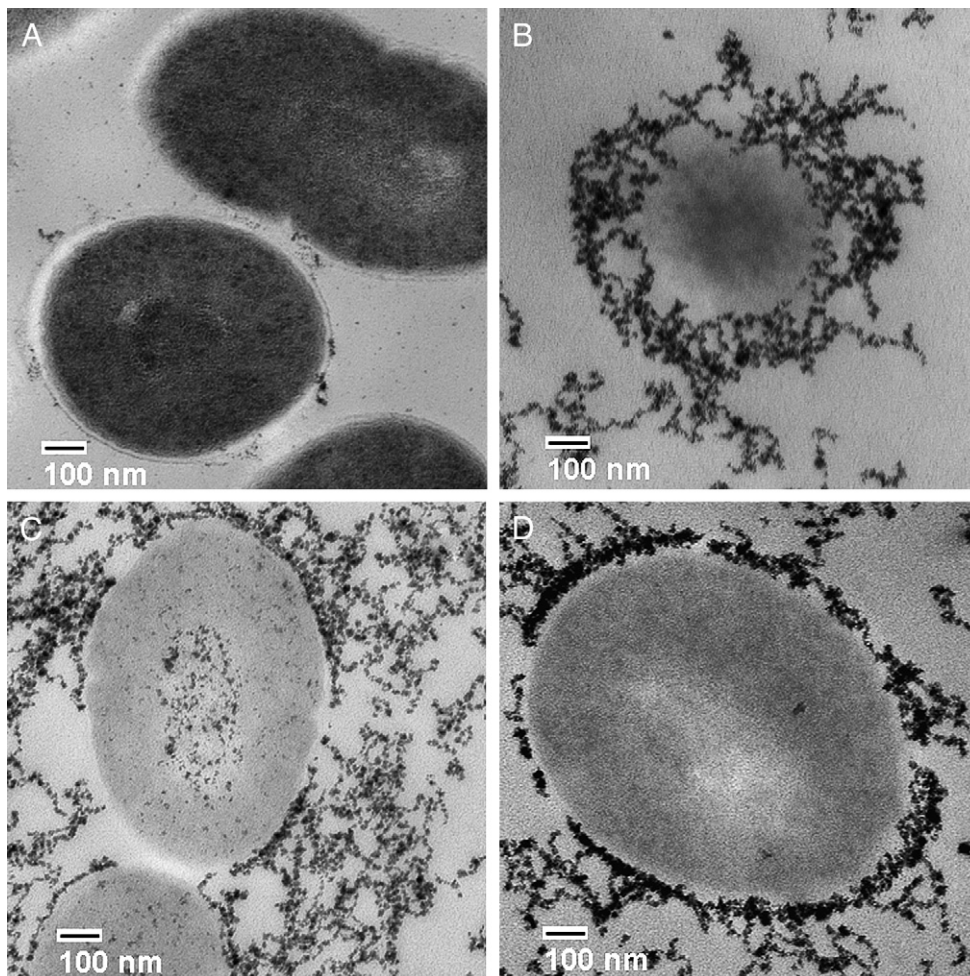


Figure 2. (A) TEM of *E. faecalis*. Colloidal gold particles complexed with poly(lactic-co-glycolic acid) are concentrated mainly on the cell walls of microorganisms after (B) 2.5 minutes, (C) 5 minutes, and (D) 10 minutes of incubation.

The bacterial suspension was collected in a 1.5-mL microcentrifuge tube positioned below the apical foramen, and bacterial yielding was measured spectrophotometrically for each sample (the reading for BHI alone was subtracted). After vortexing for 20 seconds, serial dilutions were prepared, and 100- μ L aliquots were inoculated onto blood agar and incubated anaerobically for 7 days.

Data Analysis

In three PDT experiments of bacterial suspensions, two treatments (MB-loaded nanoparticles alone and light plus MB-loaded nanoparticles) and a control were evaluated. Four observations (CFU counts) were obtained for each treatment group in each of the three experiments, a total of 12 observations per treatment and 36 observations overall. Data values were \log_{10} transformed to reduce variance heterogeneity. Treatment effects on \log_{10} CFU levels were evaluated in a two-way analysis of variance (3 experiments \times 3 treatments) in order to control any extraneous variation from experiment to experiment, while obtaining summary comparisons of treatment effects. Pair-wise comparisons of mean treatment levels were performed by the Tukey multiple comparisons procedure with an overall alpha of 0.01. In the case of the root canal data, a similar analysis was performed for \log_{10} CFU values, in this case with two experiments and again with four observations for each treatment group, a total of eight observations per treatment and 24 observations overall (two experiments \times three treatments). After analysis of variance, pair-wise comparisons of treatment effects were again performed by the Tukey procedure with an overall alpha of 0.01.

Results

Characterization of Nanoparticles

The diameter of PEO-PLGA nanoparticles ranged from 100 to 250 nm. The particle size remained the same with the inclusion of MB. The surface charge of the nanocarriers, in the absence and presence of encapsulated payload, was determined by zeta potential measurements and was found to be -23.48 and -31.87 mV, respectively. These average values were obtained from six independent batches of nanoparticles and were not statistically significant ($p > 0.05$). After freeze-drying, the surface morphology of the nanocarriers was visualized by SEM. PLGA nanoparticles were spherical in shape and had a smooth surface (Fig. 1). UV-visible spectroscopy verified the capacity and efficiency of MB encapsulation.

TEM Studies

The uptake and distribution of nanoparticles in *E. faecalis* was investigated by TEM using PLGA complexed with colloidal gold particles (10-15 nm) in order to obtain high contrast. After incubation of microorganisms with a suspension (100 μ g/mL) of PLGA-Au-Pluronic nanoparticles for up to 10 minutes, TEM revealed substantial accumulation of nanoparticles on bacterial cell walls (Fig. 2B-D). The surface properties (size and charge) of nanoparticles were the same for either gold or MB.

Photosensitization of *E. faecalis* in Planktonic Phase

Mean \log_{10} CFU levels, summarized for all three experiments in Figure 3, were highest for control, slightly lower for MB-loaded nanoparticles alone, and markedly lower for the combination of light with MB-loaded nanoparticles. This same pattern of progressively lower mean levels was observed in all three experiments. Treatment main effects in the two-way analysis of variance were highly significant ($p < 0.0001$). Pair-wise comparisons among treatment means by the

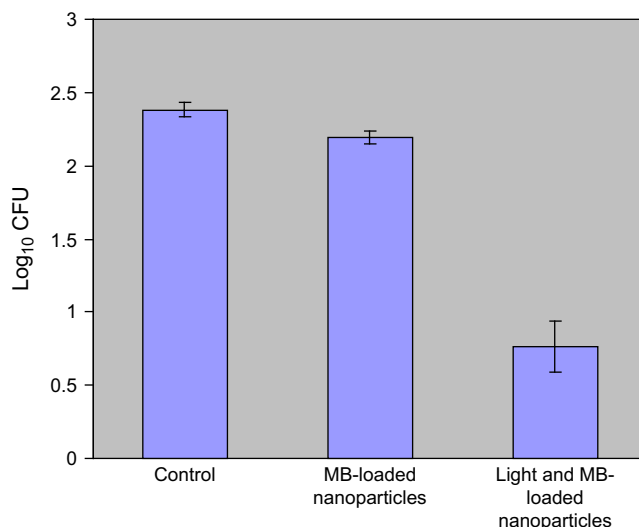


Figure 3. Phototoxicity of *E. faecalis* species after incubation with MB-loaded PLGA nanoparticles (final concentration: 6.25 μ g/mL equivalent to MB) for 10 minutes followed by treatment with red light of 665 nm (60 J/cm²) and colony-forming assay. Each bar is the mean \log_{10} CFU levels (\pm standard error). The combination of light and MB-loaded nanoparticles was significantly lower than control or MB-loaded nanoparticles alone (pair-wise comparisons of means by the Tukey procedure with an overall alpha of 0.01).

Tukey multiple comparisons procedure with an overall alpha of 0.01 indicated that MB-loaded nanoparticles were not significantly lower than control and that light with MB-loaded nanoparticles was significantly lower than both control and MB-loaded nanoparticles alone. Survival fractions relative to control levels (mean CFU = 259.5), computed separately for each experiment and then averaged over the three experiments, were 66.1% for MB-loaded nanoparticles and 3.3% for light with MB-loaded nanoparticles. In separate experiments, bacterial viability was not reduced when microorganisms were treated with either only light or only with unloaded nanoparticles (data not shown).

SEM Studies

SEM demonstrated open dentinal tubules after the removal of the smear layer with NaOCl and EDTA (Fig. 4A). Three days after inoculation with *E. faecalis*, a dense infection occurred in the root canal (Fig. 4B). SEM also showed the delivery of spherically shaped MB-loaded PLGA nanoparticles in the root canal system (Fig. 4C).

Photosensitization of Root Canal Biofilm Bacteria

Results for root canal experiments (Fig. 5) followed a similar pattern to that seen in the planktonic experiments. Treatment main effects in the two-way analysis of variance were highly significant ($p < 0.0001$). Pair-wise comparisons among treatment means with an overall alpha of 0.01 indicated that both MB-loaded nanoparticles only and light with MB-loaded nanoparticles were both significantly lower than the control. In addition, light with MB-loaded nanoparticles was significantly lower than MB-loaded nanoparticles. Survival fractions relative to mean CFU for control levels (mean CFU = 260.4) were 41.5% for MB-loaded nanoparticles and 15.2% for light with MB-loaded nanoparticles.

Discussion

Polymer-based nanoparticles have recently been used for the delivery of photosensitizers and release systems, in particular those

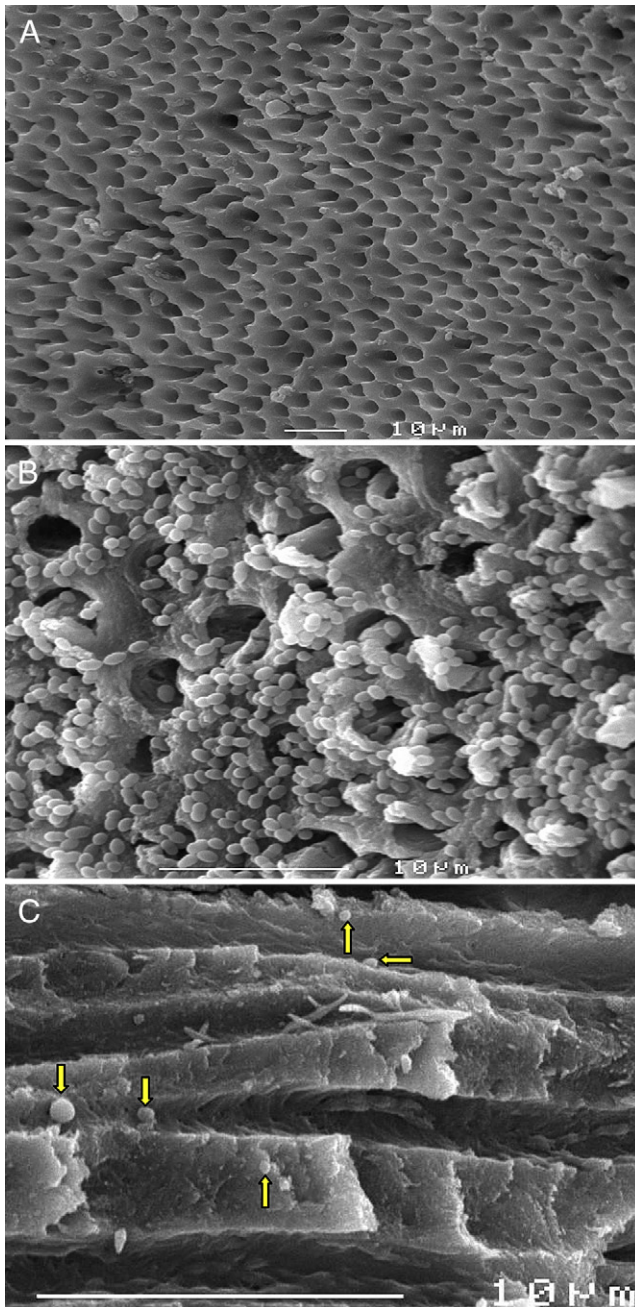


Figure 4. (A) SEM: the root canal surface with the openings of dentinal tubules before infection with *E. faecalis*. (B) *E. faecalis* biofilms on the pulpal canal wall and invasion of microorganisms into the dentinal tubules. (C) Infiltration of dentinal tubules by MB-loaded nanoparticles (arrows).

with biocompatible and biodegradable polymers. These systems are able to target different organs and control the release of the photosensitizer molecules by the incorporation of site-specific moieties (eg, the modification of the particles' surface with poly(ethylene oxide) to improve the carrier's biocompatibility and biodistribution [33–35]). The present study explored a new approach for antimicrobial therapy against the microorganism *E. faecalis* with light activation of targeted MB-loaded PLGA nanoparticles. Our goals were to investigate (1) the susceptibility of *E. faecalis* species in the planktonic phase and (2) the ability of nanoparticles to deliver MB in the root canal system and root canal biofilms of experimentally infected teeth enabling their elim-

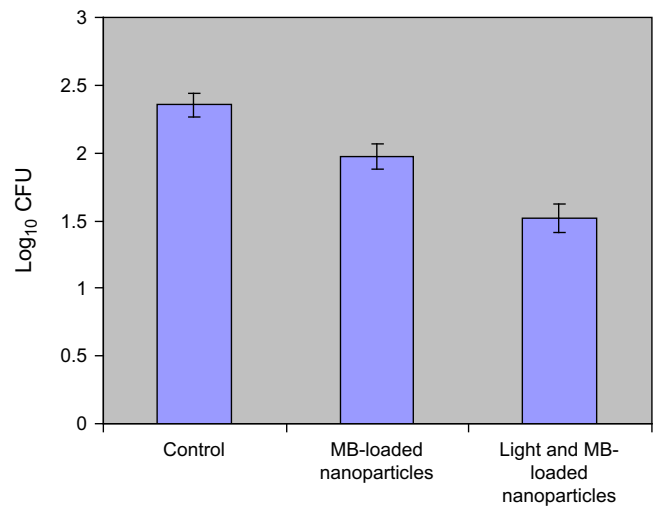


Figure 5. Phototoxicity mediated in *E. faecalis*-derived root canal biofilms after incubation with MB-loaded PLGA nanoparticles (final concentration: 50 $\mu\text{g}/\text{mL}$ equivalent to MB) for 15 minutes followed by exposure to red light of 665 nm (30 J/cm^2) and colony-forming assay. Each bar is the mean log₁₀ CFU levels (\pm standard error). The combination of light and MB-loaded nanoparticles was significantly lower than control or MB-loaded nanoparticles alone (pair-wise comparisons of means by the Tukey procedure with an overall alpha of 0.01).

ination by PDT. The nanoparticle matrix PLGA is a polyester copolymer of polylactic acid and polyglycolic acid that has received Food and Drug Administration approval because of its biocompatibility and its ability to degrade in the body through natural pathways (36). MB has previously been encapsulated into polyacrylamide, sol-gel silica, and organically modified silicate nanoparticles for phototargeting tumor cells *in vitro* (37). Recently, MB-containing silica-coated magnetic nanoparticles were proposed as potential carriers for PDT (38).

The susceptibility of *E. faecalis* species to PDT mediated by MB-loaded PLGA nanoparticles was investigated in the planktonic phase. The sensitization of *E. faecalis* species with nanoparticles (6.25 $\mu\text{g}/\text{mL}$ equivalent to MB) followed by exposure to red light at 665 nm with energy fluence of 60 J/cm^2 led to approximately 2 log₁₀ bacterial killing. In addition, the synergism of nanoparticles (50 $\mu\text{g}/\text{mL}$ equivalent to MB) and light (30 J/cm^2) exhibited approximately 1 log₁₀ killing of *E. faecalis* biofilm species in experimentally infected root canals of human extracted teeth. In both planktonic and root canal experiments, MB-loaded nanoparticles alone exhibited approximately 44% and 58% reduction of bacterial viability, respectively. In the present study, the effect of light alone in root canals was not investigated. A previous study conducted by our group did not show a significant effect of light on bacterial viability compared with controls (no light/no drug) (18). Although direct comparisons between results obtained from planktonic and root canal experiments cannot be made, both experimental conditions clearly show the bacterial susceptibility to PDT induced by MB-loaded PLGA nanoparticles. A complete evaluation of the photodynamic effects of MB-loaded nanoparticles on root canal biofilms would also require knowledge of optimum treatment parameters. These include the concentration of MB encapsulated in nanoparticles, the incubation time of nanoparticles with microorganisms, the power density, and the energy fluence of light. TEM showed that nanoparticles were mainly concentrated on bacterial cell walls. This may have rendered the cell wall permeable to MB (39) released by the nanoparticles. In this case, the intracellular localization and the local surroundings of MB influence the phototoxicity. Sensitization of MB with light leads to the

production of singlet oxygen (1O_2), which can migrate approximately 0.02 μm after its formation, targeting important intracellular components (12). There is also another scenario, according to which photodestruction takes place within the cell wall. In this case, the intracellular content may have leaked out. However, the fact that MB-loaded nanoparticles alone exhibited a toxicity ranging from 34% to 58.5% suggests that MB penetrated the bacterial cell well.

The photodynamic effects of MB-loaded PLGA nanoparticles on *E. faecalis* were probably affected by the presence of serum proteins in BHI broth (40–42). Preliminary results obtained in our laboratory from PDT studies using MB-loaded PLGA nanoparticles for targeting *E. faecalis* *in vitro* show greater bacterial killing when these nanoparticles are dissolved in PBS (unpublished data). Recently, it was found that MB dissolved in a mixture of glycerol:ethanol:water (17) as well as a MB formulation containing an emulsion of oxidizer:oxygen carrier (19) enhanced the photodynamic effects of MB *in vitro*. A limitation of the present study is related to the sampling method used for the collection of biofilm species from root canals. Flushing with medium leads to detachment of biofilm species mainly from the surface of the root canal and the openings of dentinal tubules. In preliminary studies, we used paper points, but fewer bacteria were obtained compared with flushing. We also crushed the root specimens (cryopulverization) in order to assay the fragments. The data obtained were not convincing. The flushing method was preferred over files in order to avoid bacterial destruction induced by the latter.

The use of a biodegradable polymer to synthesize the nanoparticles makes the final product attractive for clinical use. Future studies should define the treatment parameters for optimum endodontic disinfection and the therapeutic window in which microorganisms could be killed by MB-loaded nanoparticles while sparing normal cells. The role of nanoparticle surface charge on antimicrobial PDT effect should also be evaluated. At a later stage, a comparison between the photodynamic effects of MB-loaded nanoparticles and free MB would be necessary.

References

- Ørstavik D, Pitt Ford TR. Apical periodontitis. Microbial infection and host responses. In: Ørstavik D, Pitt Ford TR, eds. Essential endodontology: prevention and treatment of apical periodontitis. Blackwell Publishing Ltd Company; 1998.
- Byström A, Sundqvist G. Bacteriologic evaluation of the effect of 0.5 percent sodium hypochlorite in endodontic therapy. Oral Surg Oral Med Oral Pathol 1983;55:307–12.
- Siqueira JF Jr, Araújo MCP, Garcia PF, et al. Histological evaluation of the effectiveness of five instrumentation techniques for cleaning the apical third of root canals. J Endod 1997;23:499–502.
- Haapasalo M, Ørstavik D. *In vitro* infection and disinfection of dentinal tubules. J Dent Res 1987;66:1375–9.
- Berutti E, Marine R, Angeretti A. Penetration ability of different irrigants into dentinal tubules. J Endod 1997;23:725–7.
- Rolph HJ, Lennon A, Riggio MP, et al. Molecular identification of microorganisms from endodontic infections. J Clin Microbiol 2001;39:3282–9.
- Siqueira JF, Rocas IN. Nested PCR detection of *Centipeda periodontii* in primary endodontic infections. J Endod 2004;30:135–7.
- Foschi F, Cavrini F, Montebugnoli L, et al. Detection of bacteria in endodontic samples by polymerase chain reaction assays and association with defined clinical signs in Italian patients. Oral Microbiol Immunol 2005;20:289–95.
- Radcliffe CE, Potouridou L, Qureshi R, et al. Antimicrobial activity of varying concentrations of sodium hypochlorite on the endodontic microorganisms *Actinomyces israelii*, *A. naeslundii*, *Candida albicans* and *Enterococcus faecalis*. Int Endod J 2004;37:438–46.
- Distel JW, Hatton JF, Gillespie MJ. Biofilm formation in medicated root canals. J Endod 2002;28:689–93.
- Raab O. Über die Wirkung Fluoreszierender Stoffe auf Infusorien. Z Biol 1900;39:524–46.
- Dougherty TJ, Gomer CJ, Henderson BW, et al. Photodynamic therapy. J Natl Cancer Inst 1998;90:889–905.
- Harris F, Chatfield LK, Phoenix DA. Phenothiazinium based photosensitizers-photodynamic agents with a multiplicity of cellular targets and clinical applications. Curr Drug Targets 2005;6:615–27.

- Soukos NS, Chen PS, Morris JT, et al. Photodynamic therapy for endodontic disinfection. J Endod 2006;32:979–84.
- Foschi F, Fontana CR, Ruggiero K, et al. Photodynamic inactivation of *Enterococcus faecalis* in dental root canals *in vitro*. Lasers Surg Med 2007;39:782–7.
- George S, Kishen A. Advanced noninvasive light-activated disinfection: assessment of cytotoxicity on fibroblast versus antimicrobial activity against *Enterococcus faecalis*. J Endod 2007;33:599–602.
- George S, Kishen A. Photophysical, photochemical, and photobiological characterization of methylene blue formulations for light-activated root canal disinfection. J Biomed Opt 2007;12:034029.
- Fimple JL, Fontana CR, Foschi F, et al. Photodynamic treatment of endodontic polymicrobial infection *in vitro*. J Endod 2008;34:728–34.
- George S, Kishen A. Augmenting the antibiofilm efficacy of advanced noninvasive light activated disinfection with emulsified oxidizer and oxygen carrier. J Endod 2008;34:1119–23.
- Lim Z, Cheng JL, Lim TW, et al. Light activated disinfection: an alternative endodontic disinfection strategy. Aust Dent J 2009;54:108–14.
- Soukos NS, Socransky SS, Mulholland SE, et al. Photomechanical drug delivery into bacterial biofilms. Pharm Res 2000;17:405–9.
- Ogura MAA, Blissett R, Ruggiero K, et al. Photomechanical wave-assisted molecular delivery in oral biofilms. World J Microbiol Biotechnol 2007;23:1637–46.
- Müller P, Guggenheim B, Schmidlin PR. Efficacy of gasform ozone and photodynamic therapy on a multispecies oral biofilm *in vitro*. Eur J Oral Sci 2007;115:77–80.
- Fontana CR, Abernethy AD. The antibacterial effect of photodynamic therapy in dental plaque-derived biofilms. J Periodontol Res 2009;44:751–9.
- Tegos GP, Hamblin MR. Phenothiazinium antimicrobial photosensitizers are substrates of bacterial multidrug resistance pumps. Antimicrob Agents Chemother 2006;50:196–203.
- Koo YEL, Fan W, Hah H, et al. Photonic explorers based on multifunctional nano-platforms for biosensing and photodynamic therapy. Appl Opt 2007;46:1924–30.
- Langer R. Drug delivery and targeting. Nature 1998;392:5–10.
- Konan YN, Berton M, Gurny R, et al. Enhanced photodynamic activity of meso-tetra(4-hydroxyphenyl)porphyrin by incorporation into sub-200 nm nanoparticles. Eur J Pharm Sci 2003;18:241–9.
- McCarthy JR, Perez JM, Brückner C, et al. Polymeric nanoparticle preparation that eradicates tumors. Nano Lett 2005;5:2525–6.
- Ricci-Júnior E, Marchetti JM. Zinc(II) phthalocyanine loaded PLGA nanoparticles for photodynamic therapy use. Int J Pharm 2006;310:187–95.
- Esmaeili F, Hosseini-Nasr M, Rad-Malekshahi M, et al. Preparation and antibacterial activity evaluation of rifampicin-loaded poly lactide-co-glycolide nanoparticles. Nanomedicine 2007;3:161–7.
- Jeong YI, Na HS, Seo DH, et al. Ciprofloxacin-encapsulated poly(DL-lactide-co-glycolide) nanoparticles and its antibacterial activity. Int J Pharm 2008;352:317–23.
- Shenoy D, Little S, Langer R, et al. Poly(ethylene oxide)-modified poly(beta-amino ester) nanoparticles as a pH-sensitive system for tumor-targeted delivery of hydrophobic drugs. 1. *In vitro* evaluations. Mol Pharm 2005;2:357–66.
- Shenoy DB, Amiji MM. Poly(ethylene oxide)-modified poly(epsilon-caprolactone) nanoparticles for targeted delivery of tamoxifen in breast cancer. Int J Pharm 2005;293:261–70.
- Devalapally H, Shenoy D, Little S, et al. Poly(ethylene oxide)-modified poly(beta-amino ester) nanoparticles as a pH-sensitive system for tumor-targeted delivery of hydrophobic drugs: part 3. Therapeutic efficacy and safety studies in ovarian cancer xenograft model. Cancer Chemother Pharmacol 2007;59:477–84.
- Panyam J, Zhou WZ, Prabha S, et al. Rapid endo-lysosomal escape of poly(DL-lactide-co-glycolide) nanoparticles: implications for drug and gene delivery. FASEB J 2002;16:1217–26.
- Tang W, Xu H, Kopelman R, et al. Photodynamic characterization and *in vitro* application of methylene blue-containing nanoparticle platforms. Photochem Photobiol 2005;81:242–9.
- Tada DB, Vono LL, Duarte EL, et al. Methylene blue-containing silica-coated magnetic particles: a potential magnetic carrier for photodynamic therapy. Langmuir 2007;23:8194–9.
- Zeina B, Greenman J, Purcell WM, et al. Killing of cutaneous microbial species by photodynamic therapy. Br J Dermatol 2001;144:274–8.
- Soukos NS, Mulholland SE, Socransky SS, et al. Photodestruction of human dental plaque bacteria: enhancement of the photodynamic effect by photomechanical waves in an oral biofilm model. Lasers Surg Med 2003;33:161–8.
- Bhatti M, MacRobert A, Meghji S, et al. Effect of dosimetric and physiological factors on the lethal photosensitization of *Porphyromonas gingivalis* *in vitro*. Photochem Photobiol 1997;65:1026–31.
- Kömerik N, Wilson M. Factors influencing the susceptibility of gram-negative bacteria to toluidine blue-mediated lethal photosensitization. J Appl Microbiol 2002;92:618–23.